Brain States Encode both Perceived Emotion and the Physiological Response Induced by Visual Stimuli

Keith A. Bush, Anthony A. Privratsky, Jonathan Gardner, Melissa J. Zielinski, Clinton D. Kilts

Brain Imaging Research Center, University of Arkansas for Medical Sciences, Little Rock, AR

Brain State Hypothesis

Multivariate pattern analysis (MVPA) of functional magnetic resonance imaging (fMRI) data has critically advanced the neuroanatomical understanding of affect processing in the human brain[1-3]. Central to these advancements is the brain state, a temporally-succinct fMRI-derived pattern of neural activation, which serves as a processing unit. In this work, we explore whether the brain state exhibits a central role in affect processing by testing its ability to predict multiple independent measures of affect while also exhibiting the neuroanatomical affective encoding structures already identified in the broader literature.

Methodology

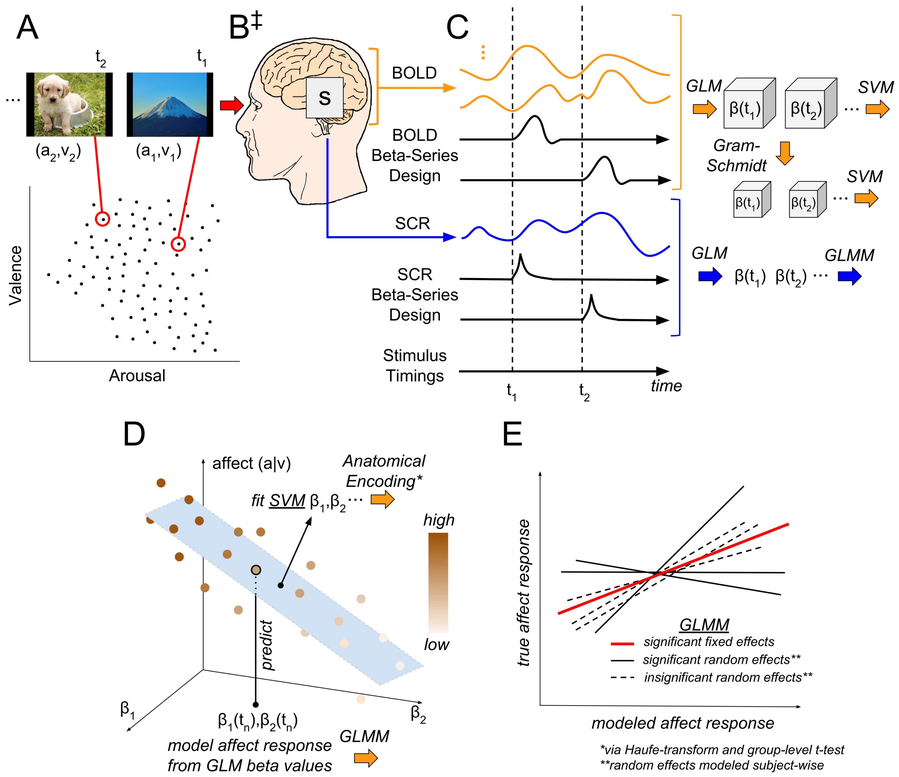

Methodological and Conceptual Overview. ***(A)*** *Experiment Design: Ninety image stimuli were selected from the International Affective Picture System (IAPS) such that the image subset exhibited the maximum span of component properties, valence (v) and arousal (a).* ***(B)*** *Signal Acquisition: Images were presented to health control subjects (n=19) for 2 s interleaved with random inter-trial intervals [2–6 s] during concurrent functional magnetic resonance imaging (fMRI) measurement of the blood oxygen level dependent (BOLD) response as well as skin conductance response (SCR).* ***(‡)*** *Conceptual Model: We hypothesis that a brain state, s, simultaneously encodes both the dimensional affective properties of each image stimulus as well as the neural impetus for its psychophysiological response.* ***(C)*** *Brain and Physiological State Estimation: 1) fMRI signals were preprocessed to remove noise and motion artifacts and segmented to remove all voxels except gray matter (GM); 2) SCR signals were preprocessed to remove noise and tonic signal components; 3) for each stimulus, neural activation patterns were extracted via the beta-series method[4]; and, 4) neural activation patterns were dimensionally reduced via Gram-Schmidt orthonormalization.* ***(D)*** *Prediction of Affective Signals:* ***The individual neural activation patterns (each matched to the labels of the stimulus from which they were derived) were used to conduct intra-subject cross-validated linear support vector machine (SVM) regression. In the example shown, the regression model predicts the affective response of a novel point (the neural activations induced by the n^{th} stimulus).*** ***(E)*** *Effect Size Estimation: Group-level predictions of affective properties and measurements were conducted via General Linear Mixed-Effects Models (GLMMs) in three tests: 1) the measurements of interest were the normative affective properties of the stimuli (v,a) and the fixed effects were the SCR measurements of affect state (β^{SCR}); 2) the measurements of interest were the affective properties (v,a) and the fixed effects were the SVM-predicted properties (~v,~a); and, 3) the measurements of interest were β^{SCR} and the fixed effects were the SVM-predicted affective responses (~β^{SCR}).* ***Individual SVM models of GM-based features were transformed into anatomical encoding representations[5] of affect state and analyzed group-wise.*** ***Random slope and intercept effects were modeled subject-wise.***

Prediction Results

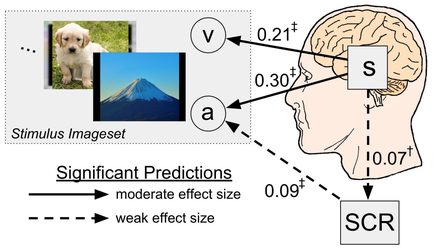

Result Figure 1 (left)*: Summary of the primary experimental findings in relation to the proposed conceptual model. Affective properties of the IAPS imageset, valence (v) and arousal (a), brain state (s), and skin conductance responses (SCR) are depicted alongside arrows indicating the direction of significant GLMM predictions (†p<0.05, ‡p<0.001, F-test), reported in units of effect size (Pearson's r).*

Result Figure 2 (below)*: Predictions of the dimensional properties of affect.* ***(A)*** *GLMM of z-scored normative valence as a function of the z-scored SVM-predicted normative valence, using Gram-Schmidt dimensionally reduced features as the model of brain state; SVM-predicted valence significantly predicts the true normative valence scores (p<0.001, F-test);* ***(B)*** *GLMM of z-scored normative arousal as a function of the z-scored SVM-predicted normative arousal using Gram-Schmidt dimensionally reduced features; SVM-predicted arousal significantly predicts the true normative arousal scores (p<0.001, F-test).* ***(C)*** *GLMM of z-scored GLM-modeled SCR activation as a function of the z-scored SVM-predicted GLM-modeled SCR activation using Gram-Schmidt dimensionally reduced features; SVM-predicted arousal significantly predicts the true normative arousal scores (p<0.05, F-test).* ***(D)*** *GLMM of z-scored normative arousal scores as a function of GLM-modeled SCR activation; SCR activation significantly predicts normative arousal (p<0.001, F-test). Circles indicate individual stimuli of the study. Red lines depict fixed-effects. Solid blue lines indicate significant random effects. Dashed blue lines indicated insignificant random effects.*

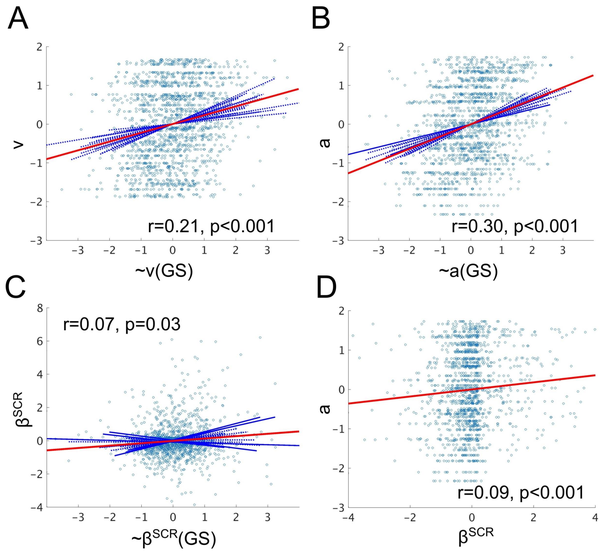

Neuroanatomical Encodings

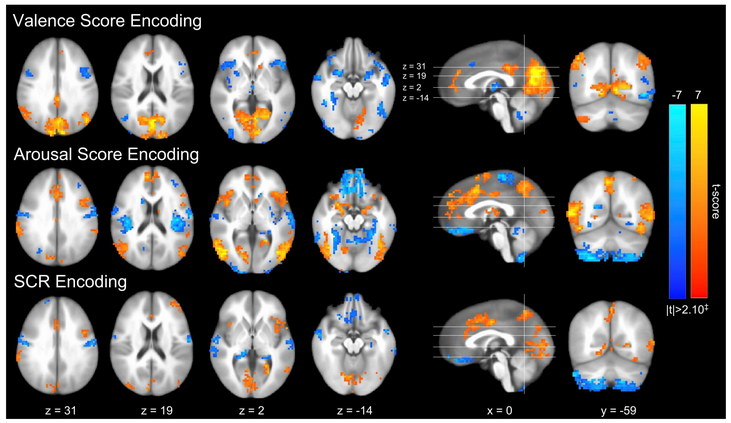

Result Figure 3 (above)*: Group-level distributions of SVM intra-subject emotion perception GM encoding parameters. Color gradations indicate the group-level strength of activations (voxel-wise t-statistic, n=19, 2-sided 1-sample t-test, null: μ=0) and the affective stimulus property for which voxel activation would be observed (red indicating positive valence or high arousal/SCR, blue indicating negative valence or low arousal/SCR). Slices are depicted in Talairach coordinate space and neurological convention. Voxel intensities are thresholded at |t|>2.10‡ (α=0.05) with maximum voxel intensity |t|=7.0. Only clusters of 20 or greater contiguous voxels (NN=1) are depicted. ‡Voxel intensities of the SCR Encoding are thresholded at |t|>2.13 (n=16, α=0.05) reflecting the omission of three participants that did not have fully acquired SCR signal. Note, a small percentage (0.003%) of voxels exhibited encoding parameters that were significantly non-normally distributed (α=0.05, Bonferroni corrected, Kolmogorov-Smirnov goodness-of-fit test).*

Result Figure 4 (right): *Quantitative group-level comparison of the cosine similarity (relative to arousal) between the neural activation encodings of arousal (a), valence (v), and skin conductance response (SCR); horizontal red segments indicate the median distribution value, upper and lower horizontal blue segments represent the 25-75% bounds of the distribution; notches indicate the range of the 95% confidence interval of the median. Neural encoding similarity is measured according to the cosine of the angle between the vectors describing the compared encoding models of the SVM hyperplanes. For each participant, the group-level similarity is formed from the group average (excluding participant) between the participant's arousal hyperplane and the comparison hyperplane. All group differences are significant (p<0.001, 2-sample Wilcoxon rank sum test, α=0.05, Bonferroni corrected for 3-way comparison, null: $\mu_1=\mu_2$). Arousal versus arousal (a vs a) and arousal versus SCR (a vs SCR) group comparisons are significantly more similar than orthogonal (p<0.001, 1-sided 1-sample Wilcoxon signed rank test, α=0.05, null: μ≤ 0) and (p<0.001, 1-sided 1-sample Wilcoxon signed rank test, α=0.05, null: μ≤ 0), respectively.*

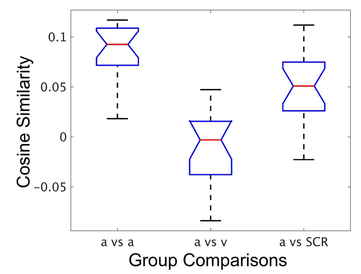

Discussion

To our knowledge, this is the first time the neural processing correlates of affective valence and arousal have been simultaneously characterized on a continuous scale in combination with a secondary validation measurement of affective reactivity. The broader value of these robust, generalizable, and predictive affective representations is their ability to measure affect processing during other tasks, e.g., emotion regulation, as well as their utility to real-time fMRI-based feedback.

Acknowledgements

The authors would like to thank Bradford Martins, Jennifer Payne, Emily Hahn, Natalie Morris, and Nathan Jones for their efforts in acquiring data as well as Sonet Smitherman and Favrin Smith for their assistance in attaining protocol approval and maintaining human subject research compliance.

Funding

Funding for this work was provided by in part by the Arkansas Science and Technology Authority (15-B-3), the Department of Psychiatry of the University of Arkansas for Medical Sciences, the National Science Foundation (BCS-1735820), and the National Institute on Drug Abuse (1R01DA036360 and 1T32DA022981).

References

1. Saarimäki, H. *et al.* Discrete Neural Signatures of Basic Emotions. *Cereb. Cortex* **26,** 2563–2573 (2016).
2. Baucom, L. B., Wedell, D. H., Wang, J., Blitzer, D. N. & Shinkareva, S. V. Decoding the neural representation of affective states. *Neuroimage* **59,** 718–727 (2012).
3. Bush, K. A., Inman, C. S., Hamann, S., Kilts, C. D. & James, G. A. Distributed Neural Processing Predictors of Multi-dimensional Properties of Affect. *Front. Hum. Neurosci.* **11,** (2017).
4. Rissman, J., Gazzaley, A. & D'Esposito, M. Measuring functional connectivity during distinct stages of a cognitive task. *Neuroimage* **23,** 752–763 (2004).
5. Haufe, S. *et al.* On the interpretation of weight vectors of linear models in multivariate neuroimaging. *Neuroimage* **87,** 96–110 (2014).